



ELSEVIER

Geomorphology 45 (2002) 89–104

GEOMORPHOLOGY

www.elsevier.com/locate/geomorph

# Using $^{10}\text{Be}$ and $^{26}\text{Al}$ to determine sediment generation rates and identify sediment source areas in an arid region drainage basin

Erik M. Clapp<sup>a,\*</sup>, Paul R. Bierman<sup>a</sup>, Marc Caffee<sup>b</sup>

<sup>a</sup>*School of Natural Resources and Department of Geology, University of Vermont, Burlington, VT 05405, USA*

<sup>b</sup>*Center for Accelerator Mass Spectrometry, Lawrence Livermore National Laboratory, Livermore, CA 94550, USA*

Received 20 September 1999; received in revised form 3 October 2000; accepted 14 October 2001

## Abstract

We measured  $^{10}\text{Be}$  and  $^{26}\text{Al}$  in 64 sediment and bedrock samples collected throughout the arid, 187 km<sup>2</sup> Yuma Wash drainage basin, southwestern Arizona. From the measurements, we determine long-term, time-integrated rates of upland sediment generation ( $81 \pm 5 \text{ g m}^{-2} \text{ year}^{-1}$ ) and bedrock equivalent lowering ( $30 \pm 2 \text{ m Ma}^{-1}$ ) consistent with other estimates for regions of similar climate, lithology, and topography. In a small ( $\sim 8 \text{ km}^2$ ), upland sub-basin, differences in nuclide concentrations between bedrock outcrops and hillslope colluvium suggest weathering of bedrock beneath a colluvial cover is a more significant source of sediment ( $40 \times 10^4 \text{ kg year}^{-1}$ ) than weathering of exposed bedrock surfaces ( $10 \times 10^4 \text{ kg year}^{-1}$ ). Mixing models constructed from nuclide concentrations of sediment reservoirs identify important sediment source areas. Hillslope colluvium is the dominant sediment source to the upper reaches of the sub-basin channel; channel cutting of alluvial terraces is the dominant source in the lower reaches. Similarities in nuclide concentrations of various sediment reservoirs indicate short sediment storage times ( $< 10^3$  years). Nuclide concentrations, measured in channel sediment from tributaries of Yuma Wash and in samples collected along the length of the Wash, were used to construct mixing models and determine sediment sources to the main stem channel. We find an exponential decrease in the channel nuclide concentrations with distance downstream, suggesting that as much as 40% of sediment discharged from Yuma Wash has been recycled from storage within basin fill alluvium. Sediment generation and denudation rates determined from the main stem are greater (25%) than rates determined from upland sub-basins suggesting that, currently, sediment may be exported from the basin more quickly than it is being generated in the uplands. Independence of nuclide concentration and sediment grain size indicates that channels transport sediment in discrete pulses before rapidly depositing poorly sorted material, suggesting that differences in transport times for different size materials are minimal. © 2002 Elsevier Science B.V. All rights reserved.

*Keywords:* Arid region sediment transport; Cosmogenic dating; Denudation; Desert geomorphology; Sediment mixing models; Sediment yield

## 1. Introduction

Estimating rates of erosion, sediment generation, and landscape change is important for understanding the effects of humans, climate, and tectonics on landscapes over both historic and geologic time scales. Concentrations of in situ-produced cosmogenic  $^{10}\text{Be}$

\* Corresponding author. Present address: C/O SME, 4 Blanchard Road Box 85A, Cumberland Center, Maine 04021, USA. Tel.: +1-207-829-5016, fax: +1-207-829-5692.

E-mail address: emc@smemaine.com (E.M. Clapp).

and  $^{26}\text{Al}$ , measured in sediment, have been used to estimate basin-wide rates of erosion and sediment generation within drainage basins (Brown et al., 1995a; Bierman and Steig, 1996; Granger et al., 1996; Small et al., 1999; Clapp et al., 2000, 2001). These studies generally focus on small (several  $\text{km}^2$  or less), lithologically homogenous, geomorphically uncomplicated basins. Three of these studies included an independent means of confirming the nuclide-based erosion rate calculation. Although the rates of sediment generation determined in these basins appear valid locally, regional estimates of erosion and denudation require the investigation of larger ( $> 100 \text{ km}^2$ ), generally more geologically and geomorphically complex basins. The techniques and interpretation methods developed in these small, controlled studies have yet to be tested in larger, more complex basins, where the processes operating to generate, transport, and store sediment are likely different than those in small, simple, upland basins.

We measured  $^{10}\text{Be}$  and  $^{26}\text{Al}$  in sediment and bedrock from the  $187 \text{ km}^2$  Yuma Wash drainage basin in southwestern Arizona (Fig. 1), to determine long-term, time-integrated rates of sediment generation and bedrock-equivalent lowering (denudation), identify sediment source areas and mechanisms of sediment delivery, and evaluate the effects of basin scale on the interpretation of cosmogenic nuclide concentrations measured in sediment. Long-term sediment generation and denudation rate estimates for large-scale basins are usually based on extrapolation, assuming steady-state, of measured short-term sediment loads (Judson and Ritter, 1964; Judson, 1968; Ahnert, 1970; Saunders and Young, 1983; Pinet and Souriau, 1988). However, when these extrapolations are used to infer sediment generation rates over thousands of years, significant errors in estimates of long-term rates are inevitable (Meade, 1969, 1988; Trimble, 1977).

$^{10}\text{Be}$  and  $^{26}\text{Al}$  are produced in quartz from the interaction of secondary cosmic rays (primarily high-

energy neutrons) with Si and O (Lal, 1988). These cosmogenic radionuclides accumulate most rapidly in sediment and bedrock residing at or near Earth's surface ( $< 3 \text{ m}$  depth); nuclide accumulation or "production" rates decrease exponentially with depth (Lal, 1988). An inverse relationship exists between the rate at which sediment is being generated and transported from a drainage basin (erosion) and the concentration of in situ-produced cosmogenic nuclides in that sediment (Lal, 1991; Brown et al., 1995a; Bierman and Steig, 1996; Granger et al., 1996). Cosmogenic nuclides present in sediment inherently integrate erosion rates over long periods of time ( $\geq 10^3$  years) and over large spatial scales. Thus, they are promising monitoring tools for the estimation of long-term rates of sediment generation (Brown et al., 1995a; Bierman and Steig, 1996; Granger et al., 1996; Small et al., 1999; Clapp et al., 2000, 2001).

In this work, we apply the techniques developed for determining basin-wide sediment generation rates in small basins (Brown et al., 1995a; Bierman and Steig, 1996; Granger et al., 1996; Small et al., 1999; Clapp et al., 2000, 2001), to both the entire Yuma Wash drainage and to smaller sub-basins of the Wash. Inconsistencies in rates determined at the two scales reflect scale-related differences in the relative importance of sediment generation, transport, and storage processes. Tracing nuclide concentrations in sediment along the length of Yuma Wash, we identify significant sediment source areas. In small-scale, upland channels, alluvium is supplied primarily from hillslope colluvium and erosion of bedrock outcrops. Along the main stem, incised channels derive much of their sediment load from erosion of basin alluvium stored in terraces, the beveled toes of long-inactive alluvial fans. Nuclide concentrations in upland basins represent the production rate of sediment from the weathering of bedrock (sediment generation). Nuclide concentrations in main stem samples reflect both upland sediment generation and the long-term effects of sediment storage and reworking.

Fig. 1. Yuma Wash drainage basin located along the Colorado River in southwestern Arizona. (A) Sample locations and  $^{10}\text{Be}$  concentrations measured in channel alluvium (enclosed in squares). Average  $^{10}\text{Be}$  concentrations (**bold**) are plotted with sample identification numbers below in parentheses. Along the main stem, nuclide concentrations decrease closer to the confluence with the Colorado River. Geology adapted from Reynolds (1988). (B) Map of southwest sub-basin with locations of bedrock, hillslope colluvium, basin fill, and channel alluvium samples. Contour interval is 100 ft, ranging from 400 to 1200 ft-msl. Base maps adapted from Ayers-Associates (1996).



## 2. Geomorphic setting

Yuma Wash, an ephemeral tributary to the Colorado River, is located in the Sonoran Desert of southwestern Arizona (Fig. 1). The wash drains a 187-km<sup>2</sup> basin that ranges in elevation from 823 m above mean sea level (m-msl) at Mojave Peak in the north, to 56 m-msl at the confluence with the Colorado River in the south. The braided channel of Yuma Wash extends approximately 26 km and reaches a maximum width of nearly 600 m.

Precipitation in the basin (91 mm year<sup>-1</sup> on average) is characterized by short but intense, localized, convective storms, during which most of the sediment transport within the basin occurs (Ayers-Associates, 1996). Stream flow and sediment transport within the wash occur as rapidly moving flood waves. For most runoff events, stream waters quickly infiltrate the alluvium upon which Yuma Wash flows, rather than flowing continuously to the Colorado River.

Yuma Wash drainage basin is underlain by Tertiary volcanic bedrock (primarily rhyolite) in the north and east, and intrusive Jurassic granites in the south and west (Reynolds, 1988). The rhyolitic rocks are highly competent and erosion resistant. Quartz content of the rhyolite is generally low (<5%) yet quartz veins provide sufficient material for separation of quartz and chemical isolation of in situ-produced cosmogenic <sup>10</sup>Be and <sup>26</sup>Al. In contrast, the granitic rocks to the south are highly weathered and generally contain >10% quartz.

The Yuma Wash drainage basin is bordered by the Chocolate Mountains to the east and north, and by the Trigo Mountains to the west (Fig. 1). Between the Chocolate and Trigo Mountains, large, coalescing and highly dissected alluvial fans occupy the valley floor (Fig. 2). The fan deposits (maximum thickness >10 m; Ayers-Associates, 1996) consist of inter-bedded debris flows, mudflows, and fluvial gravels, which are incised by Yuma Wash and its tributaries. These alluvial deposits cover between 60% and 70% of the drainage basin. Well-developed desert pavements and darkly varnished pebbles and cobbles cover parts of the fans, indicating that some surfaces are stable over time periods in excess of several thousand years. Fan deposits in Yuma Wash are believed to correlate with middle to late Pleistocene surfaces found elsewhere in the region (Dohrenwend et al., 1991), although no numerical chronology has been established, and no <sup>14</sup>C datable material was found during this study. Some of the fan deposits appear to have been tilted and beveled, suggesting that they might be much older.

The southwest sub-basin (Figs. 1 and 3) is characterized by the steep (10° to 30°), weathered, granitic slopes of the Trigo Mountains. Elevations in the sub-basin range from 354 to 122 m-msl. Much of the sub-basin (~70%) are slopes mantled with very thin colluvium (generally <20 cm). The upper 40% (by area) of the basin has little sediment storage with the exception of 2- to 3-m thick colluvial deposits at the base of some steep slopes; channel sediments of the upper wash are likely derived directly from down-



Fig. 2. Photograph of main stem of Yuma Wash. Rhyolitic uplands of the Chocolate Mountains in background. Large coalescing and incised fans with varnished surfaces are in the foreground to the left of the braided channel. View is approximately 6 km across, looking downstream (south). Photograph taken near YPG-17.



Fig. 3. Photograph of southwest sub-basin illustrating steep, granitic, upland sections with little sediment storage. View in photograph is approximately 1 km across, looking upstream (west).

slope transport of hillslope colluvium. Lower in the sub-basin, sediment storage becomes more significant where a transition from the steep upper basin terrain to the coalescing fan terrain of the main wash occurs. The lower reaches of the southwest fork cuts through poorly consolidated material 2- to 10-m thick. These materials consist of interbedded deposits of fluvial gravels from the channel and colluvial deposits from the hillslopes above.

### 3. Methods

#### 3.1. Sample collection

Samples were collected to quantify cosmogenic nuclide concentrations throughout Yuma Wash and the southwest fork sub-basin (Table 1). Samples of channel sediment were collected from immediately above the

junction of eight tributaries to Yuma Wash and at five locations along the main stem of the wash (Fig. 1). This sampling strategy allows for an interpretation of relative sediment contributions from each of the tributaries through the use of mixing models. Each of the channel samples is an integration of smaller samples taken at  $\sim 1$  m intervals across the wash. We collected our samples from the top 10 cm of the channel sediment.

In the southwest sub-basin, we collected three samples from upland granitic outcrops, three composite samples of hillslope colluvium, two depth profiles of the basin alluvium, and five homogenized samples of the active channel sediments (Fig. 1). The granite samples were collected from ridges surrounding the sub-basin. The hillslope colluvium samples were collected on three different hillslopes; each was an integration of evenly spaced ( $\sim 1$  m) samples taken along  $\sim 100$  m downslope transects YPG-23, 24, and 25 (Fig. 1). Each of the hillslope transect samples was also an integration of the total depth (10 to 20 cm) of hillslope colluvium. We assumed complete mixing of sediment would occur for such shallow cover.

Two depth profiles were sampled where the southwest fork cuts through the interbedded alluvial and colluvial deposits (Fig. 1). Four sediment samples were collected (each integrated over a 10-cm depth range) from an 8-m-deep profile at sample location YPG-10. The profile samples were taken 2, 4, 6, and 8 m below the ground surface. A similar profile (YPG-26) was sampled 1400 m down stream. Sediment samples here were taken 1.5, 2.5, and 3.5 m below the surface of the 3.5-m-deep channel cut.

#### 3.2. Sample preparation

Sediment samples were dry sieved into seven size fractions ( $<250$ ,  $<500$ ,  $<1000$ ,  $<2000$ ,  $<4000$ ,  $<12,700$ , and  $>12,700$   $\mu\text{m}$ ) and weighed. Particles smaller than 250  $\mu\text{m}$  were not used for isotopic analysis in order to minimize the effect of potential aeolian contributions from outside the basin. Samples YPG-2 and YPG-19 were used for a detailed nuclide versus grain size evaluation. For sample YPG-2, all six grain-size fractions greater than 250  $\mu\text{m}$  were analyzed separately. For YPG-19, the 1000 to 2000 and 2000 to 4000  $\mu\text{m}$  fractions had to be combined to make one sample and the 4000 to 12,700 and  $>12,700$   $\mu\text{m}$  fractions were combined to make another sample, due

Table 1  
 (A) Locations and descriptions of samples from Yuma Wash, Arizona for samples with multiple grain sizes

Sample	Average elevation <sup>a</sup> of basin (km)	Sample description	Grain size (μm)	%Sample mass	<sup>10</sup> Be (10 <sup>5</sup> atoms g <sup>-1</sup> )	<sup>10</sup> Be average <sup>b</sup> ± standard error (10 <sup>5</sup> atoms g <sup>-1</sup> )	<sup>26</sup> Al (10 <sup>5</sup> atoms g <sup>-1</sup> )	<sup>26</sup> Al average <sup>b</sup> ± standard error (10 <sup>5</sup> atoms g <sup>-1</sup> )
YPG 2A	0.366	main stem channel sediment	250–500	16	1.11 ± 0.09		6.54 ± 0.35	
YPG 2B			500–1000	8	1.39 ± 0.10		7.98 ± 0.46	
YPG 2C			1000–2000	16	1.08 ± 0.08		7.69 ± 0.44	
YPG 2D			2000–4000	18	1.18 ± 0.10		6.62 ± 0.42	
YPG 2E			4000–12,700	30	0.99 ± 0.13		7.11 ± 0.52	
YPG 2F			>12,700	12	1.09 ± 0.12	1.10 ± 0.06	6.32 ± 0.39	7.00 ± 0.27
YPG 4A	0.366	main stem channel sediment	250–1000	34	1.15 ± 0.11		6.46 ± 0.38	
YPG 4B			1000–4000	66	1.34 ± 0.11	1.28 ± 0.10	7.63 ± 0.74	7.24 ± 0.58
YPG 10.3A	0.178	sub-basin fill	250–1000	8	1.25 ± 0.10		7.96 ± 0.48	
YPG 10.3B			1000–4000	32	1.21 ± 0.07		7.85 ± 0.47	
YPG 10.3C			>4000	60	1.15 ± 0.08	1.18 ± 0.03	7.65 ± 0.53	7.74 ± 0.09
YPG 10.5A	0.178	sub-basin fill	250–1000	11	1.15 ± 0.11		7.68 ± 0.53	
YPG 10.5B			1000–4000	36	1.47 ± 0.11		6.74 ± 0.71	
YPG 10.5C			>4000	53	1.36 ± 0.11	1.38 ± 0.09	8.47 ± 1.31	7.76 ± 0.50
YPG 10.7A	0.178	sub-basin fill	250–1000	10	0.26 ± 0.20		8.61 ± 0.72	
YPG 10.7B			1000–4000	34	1.03 ± 0.11		6.92 ± 0.86	
YPG 10.7C			>4000	56	1.07 ± 0.10	0.98 ± 0.26	7.08 ± 0.54	7.18 ± 0.54
YPG 10.9A	0.178	sub-basin fill	250–1000	4	1.19 ± 0.15		10.33 ± 0.76	
YPG 10.9B			1000–4000	14	1.15 ± 0.11		7.82 ± 0.56	
YPG 10.9C			>4000	82	1.02 ± 0.09	1.04 ± 0.05	7.85 ± 0.53	7.94 ± 0.83
YPG 11B	0.241	sub-basin channel sediment	1000–4000	25	1.51 ± 0.07		na	na
YPG 11C			>4000	75	1.70 ± 0.09	1.65 ± 0.09	na	na
YPG 12A	0.241	sub-basin channel sediment	250–1000	7	1.39 ± 0.10		9.12 ± 0.70	
YPG 12B			1000–4000	37	1.38 ± 0.07		9.30 ± 0.60	
YPG 12C			>4000	56	1.32 ± 0.09	1.35 ± 0.02	8.69 ± 1.04	8.95 ± 0.18
YPG 13A	0.241	sub-basin channel sediment	250–1000	8	1.36 ± 0.11		9.43 ± 0.66	
YPG 13B			1000–4000	37	1.58 ± 0.08		8.96 ± 0.49	
YPG 13C			>4000	55	1.78 ± 0.10	1.67 ± 0.12	15.77 ± 4.45	12.74 ± 2.20
YPG 14A	0.178	sub-basin channel sediment	250–1000	10	1.20 ± 0.08		8.50 ± 0.62	
YPG 14B			1000–4000	31	1.30 ± 0.05		7.43 ± 0.71	
YPG 14C			>4000	59	1.22 ± 0.06	1.24 ± 0.03	8.11 ± 0.50	7.94 ± 0.31
YPG 15A	0.178	sub-basin channel sediment	250–1000	15	1.20 ± 0.07		na	na
YPG 15B			1000–4000	37	1.22 ± 0.11		na	na
YPG 15C			>4000	48	1.35 ± 0.06	1.28 ± 0.05	na	na
YPG 19A	0.545	main stem channel sediment	250–500	7	1.77 ± 0.10		11.19 ± 0.90	
YPG 19B			500–1000	9	1.93 ± 0.09		11.37 ± 0.58	
YPG 19C			1000–4000	33	2.06 ± 0.09		12.33 ± 0.76	
YPG 19F			4000–>12,700	51	1.63 ± 0.08	1.81 ± 0.09	10.90 ± 1.21	11.44 ± 0.31

YPG 26.1A	0.178	sub-basin fill	250–1000	5	1.27 ± 0.08		7.63 ± 0.41	
YPG 26.1B			1000–4000	24	1.22 ± 0.06		7.66 ± 0.41	
YPG 26.1C			>4000	71	1.28 ± 0.07	1.26 ± 0.02	7.22 ± 0.92	7.34 ± 0.14
YPG 26.2A	0.178	sub-basin fill	250–1000	4	1.23 ± 0.11		7.96 ± 0.55	
YPG 26.2B			1000–4000	36	1.23 ± 0.08		7.40 ± 0.44	
YPG 26.2C			>4000	60	1.08 ± 0.06	1.14 ± 0.05	7.18 ± 0.42	7.29 ± 0.23
YPG 26.3A	0.178	sub-basin fill	250–1000	7	1.17 ± 0.08		6.83 ± 0.63	
YPG 26.3B			1000–4000	25	1.19 ± 0.07		6.71 ± 0.40	
YPG 26.3C			>4000	68	1.15 ± 0.06	1.16 ± 0.01	7.65 ± 0.45	7.36 ± 0.29

(B) Locations and descriptions of samples from Yuma Wash, Arizona for samples with single grain size

Sample	Elevation <sup>c</sup> (km)	Average elevation <sup>a</sup> of basin (km)	Sample description	Grain size (microns)	<sup>10</sup> Be (10 <sup>5</sup> atoms g <sup>-1</sup> )	<sup>26</sup> Al (10 <sup>5</sup> atoms g <sup>-1</sup> )
YPG 2Q <sup>d</sup>	0.067	0.366	main stem channel quartz clast	>12,700	0.50 ± 0.10	2.77 ± 0.24
YPG 3A	0.140	0.366	main stem channel sediment	250–1000	1.16 ± 0.07	6.97 ± 0.58
YPG 5A	0.129	0.366	main stem channel sediment	250–1000	1.36 ± 0.07	6.83 ± 0.41
YPG 7	0.323	na	bedrock	na	3.21 ± 0.14	20.77 ± 1.14
YPG 8	0.344	na	bedrock	na	2.25 ± 0.11	12.60 ± 0.70
YPG 9	0.283	na	bedrock	na	2.73 ± 0.15	14.46 ± 0.58
YPG 16A	0.143	0.496	main stem channel sediment	250–1000	0.84 ± 0.05	4.69 ± 0.39
YPG 17A	0.177	0.513	main stem channel sediment	250–1000	1.54 ± 0.06	8.93 ± 0.55
YPG 18A	0.223	0.536	main stem channel sediment	250–1000	1.56 ± 0.06	9.42 ± 0.54
YPG 20A	0.259	0.554	main stem channel sediment	250–1000	1.92 ± 0.11	11.55 ± 0.79
YPG 21A	0.256	0.554	main stem channel sediment	250–1000	2.19 ± 0.08	14.34 ± 0.84
YPG 22A	0.262	0.554	main stem channel sediment	250–1000	1.53 ± 0.14	9.10 ± 1.17
YPG 23	0.207	0.187	hillslope colluvium	250–1000	1.16 ± 0.06	7.56 ± 0.56
YPG 24	0.207	0.187	hillslope colluvium	250–1000	1.32 ± 0.05	8.01 ± 0.47
YPG 25	0.075	0.187	hillslope colluvium	250–1000	1.66 ± 0.05	11.00 ± 0.65
YPG 27	0.238	0.543	main stem channel sediment	250–1000	1.66 ± 0.09	10.39 ± 0.53
YPG 28	0.293	0.547	main stem channel sediment	250–1000	2.16 ± 0.10	14.22 ± 0.73

Letters indicate multiple grain sizes analyzed at a sampling location.

Numbers following decimals indicate sample order in depth profiles (i.e. YPG 26.3 was the third sample from top of profile).

All sample location latitudes ~ N33°05'.

na (not applicable) indicates no sample results.

<sup>a</sup> Weighted average elevation of drainage basin above the sample location (represents possible elevations of sediment source).

<sup>b</sup> Average and standard error of the mean of grain-size fractions at each sampling location, weighted by mass%.

<sup>c</sup> Measured using Garmin 75 handheld GPS, verified with USGS topographic map.

<sup>d</sup> YPG-2Q is a single quartz clast from sample YPG-2.

to small sample sizes. The size fractions for twelve of the sediment samples from the southwest sub-basin were recombined according to their weight percentages to yield three composite size fractions (250 to 1000, 1000 to 4000, and >4000  $\mu\text{m}$ ) to test nuclide concentration dependence on grain size. Bedrock samples and the previously sieved sediment samples greater than 1000  $\mu\text{m}$  were crushed and sieved to yield optimal particle sizes for sample processing of 250 to 1000  $\mu\text{m}$ . The remaining 13 sediment samples were sieved to yield only the 250 to 1000  $\mu\text{m}$  size fraction that was used for analysis.

All samples were heated and ultrasonically etched, once in 6N HCl and then repeatedly in 1% HF and 1% HNO<sub>3</sub> in order to isolate 20 to 30 g of pure quartz and remove any atmospheric <sup>10</sup>Be (Kohl and Nishiizumi, 1992). The samples were then dissolved using HF and the Be and Al were isolated using ion chromatographic techniques. For all samples, 250  $\mu\text{g}$  of Be carrier was added prior to digestion. <sup>10</sup>Be/<sup>9</sup>Be and <sup>26</sup>Al/<sup>27</sup>Al ratios were determined by accelerator mass spectrometry at Lawrence Livermore National Laboratory. <sup>10</sup>Be and <sup>26</sup>Al concentrations were then calculated from known amounts of <sup>9</sup>Be (measured amount added as carrier) and <sup>27</sup>Al (native to the quartz and measured in duplicate aliquots by Inductively Coupled Argon Plasma Spectrometry–Optical Emission).

### 3.3. Data interpretation

Measurements of both <sup>10</sup>Be and <sup>26</sup>Al provide a verification of laboratory methods and constrain the exposure history of the samples we analyzed. Measured ratios ( $\mu = 5.98 \pm 0.32$ ) of <sup>26</sup>Al to <sup>10</sup>Be (Fig. 4) are consistent with the currently accepted production ratio of  $\sim 6:1$  (Nishiizumi et al., 1989), indicating that our laboratory methods are robust, and that the sediment and bedrock we sampled do not have long-term (>100 ka), complex histories of burial and exhumation. Because the two isotopes are well correlated, we present primarily the <sup>10</sup>Be measurements in Section 4. However, the <sup>26</sup>Al measurements included in Table 1 have been used in all erosion rate calculations we present.

Production rates of 6.03 and 36.8 (atoms g<sup>-1</sup> year<sup>-1</sup>) for <sup>10</sup>Be and <sup>26</sup>Al, respectively (Nishiizumi et al., 1989), scaled for latitude and elevation according to Lal (1991) and assuming no muon production (Brown et al., 1995b) and 20% uncertainty (Clark et al., 1995), were used in calculation of erosion rates. No corrections have been made for quartz enrichment (Small et al., 1999). All statistical comparisons were made using a confidence interval of 90% and independent, *t*-tests assuming unequal variance (Ott, 1993).

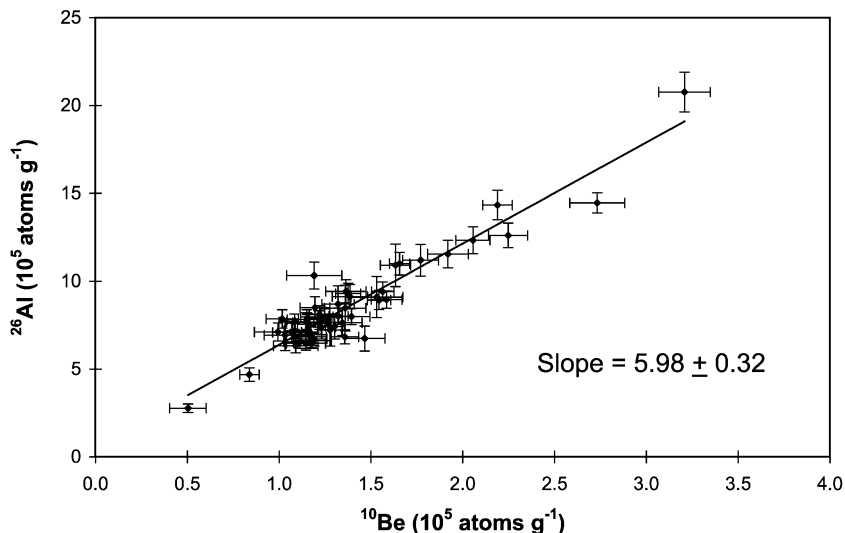


Fig. 4. <sup>10</sup>Be and <sup>26</sup>Al concentrations for all Yuma Wash samples. Least squares best fit line has a slope of  $5.98 \pm 0.32$ , and y-intercept near zero ( $0.40 \pm 0.24$ ) consistent with the currently accepted production ratio of  $\sim 6:1$  (Nishiizumi et al., 1989).

#### 4. Results and discussion

Analyses of  $^{10}\text{Be}$  and  $^{26}\text{Al}$  from both the small, southwest sub-basin and the larger, Yuma Wash drainage basin, provide considerable information about drainage basin dynamics. Southwest sub-basin data allow us to determine important sources of sediment and understand better the processes of upland sediment generation (regolith production) by comparing nuclide concentrations measured in specific geomorphic features. Main stem Yuma Wash data allow us to determine areas of significant sediment yield, including entire sub-basins and sediment stored in fans and terraces. Integration of the data collected at both scales identifies scale-related differences in basin dynamics.

##### 4.1. Grain size

Samples collected in both the southwest sub-basin and along the main stem of Yuma Wash demonstrate that nuclide concentrations are independent of sediment grain size. Within the southwest sub-basin, three grain-size fractions combined from 12 samples, give nearly identical mean concentrations (Fig. 5). Standard deviations increase with grain size as the number of

particles analyzed per unit weight of sample decreases. Two samples (YPG-2 and YPG-19) from along the main stem of Yuma Wash, divided into six and four grain-size fractions, respectively, also show no grain size-related trends in nuclide concentrations (Fig. 6). In addition, we analyzed separately a single quartz clast ( $\sim 55$  mm diameter) from sample YPG-2. Measurement of the single clast (YPG-2Q) illustrates the idiosyncratic history of clasts and utility of averaging many particles as opposed to measuring a single particle. We find that YPG-2Q has  $^{10}\text{Be}$  and  $^{26}\text{Al}$  concentrations ( $0.50 \pm 0.10$  and  $2.77 \pm 0.24 \times 10^5$  atoms  $\text{g}^{-1}$ ) that are less than half the average for all other YPG-2 samples ( $1.10 \pm 0.06$  and  $7.0 \pm 0.27 \times 10^5$  atoms  $\text{g}^{-1}$ ).

Independence of nuclide concentration and grain size implies that both large and small particles are produced by similar processes and transported at similar rates. This finding contrasts with that of Brown et al. (1995a) who found distinct isotopic dependence on grain size in a humid region where deep-seated landslides and rockslides bring large-grained, lightly dosed material to the channel while fine- to medium-grained material with higher isotopic concentrations is delivered to the stream by gradual, surface-dominated

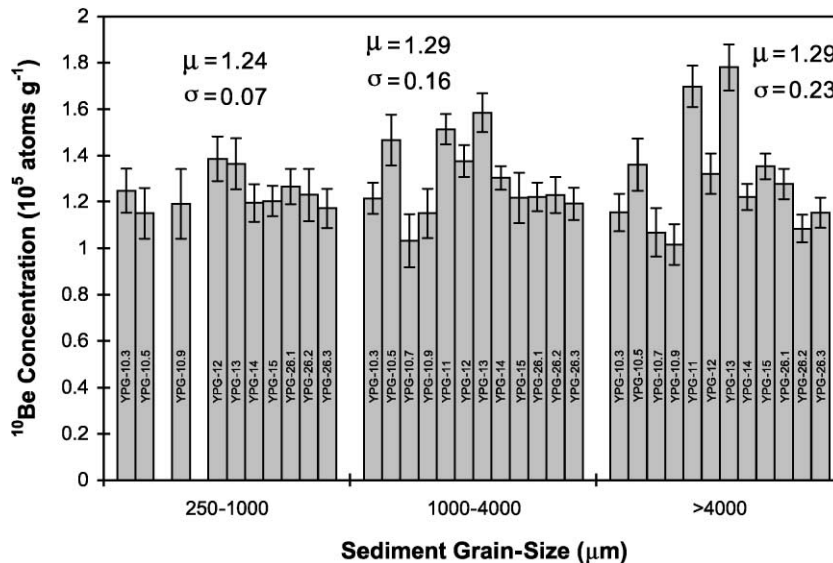


Fig. 5. Sediment grain size versus  $^{10}\text{Be}$  concentration for all sediment samples analyzed. Error bars represent laboratory analytical error. Mean nuclide concentration is similar for the three grain-size fractions. Variability increases with increasing grain size because the number of particles analyzed for coarser-grained material is less than the number analyzed for finer-grained material.

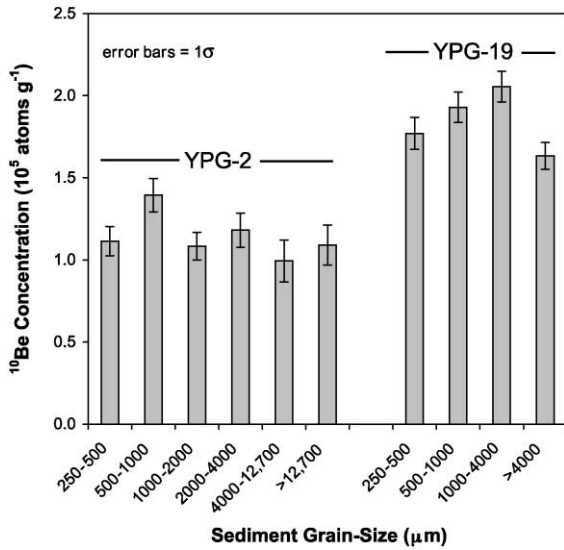


Fig. 6. Sediment grain size versus  $^{10}\text{Be}$  concentration for YPG-2 (six size fractions) and YPG-19 (four size fractions). There are no grain size-related trends in nuclide concentrations.

processes of weathering, soil creep, and sheet wash. In Yuma Wash, sediment is generally delivered to the channel by surficial rather than deep-seated processes.

Consistent with arid-region sediment transport theory, we observed no dependence of sediment nuclide concentrations on grain size. Sediment transport in ephemeral streams of arid regions often occurs in pulses during infrequent, large, storm events. The intense nature of these transport events is characterized by turbulent flows which transport material of many different sizes at similar rates

(Laronne and Reid, 1993; Laronne et al., 1994; Reid and Laronne, 1995). These flows often infiltrate the channel after short distances; flow duration is insufficient to armor the bed or selectively transport finer grain sizes.

#### 4.2. Southwest sub-basin

Detailed sampling of the southwest sub-basin provides insight into the generation and transport of sediment in a small, upland, arid drainage basin. The  $^{10}\text{Be}$  concentrations measured in bedrock outcrops ( $2.73 \pm 0.28 \times 10^5 \text{ atoms g}^{-1}$ ,  $n=3$ ) were high (Table 2) compared to those measured in hillslope colluvium ( $1.38 \pm 0.15 \times 10^5 \text{ atoms g}^{-1}$ ,  $n=3$ ). This result suggests that weathering of bedrock beneath a cover of colluvium is more rapid (less nuclide accumulation) than weathering of exposed bedrock. This observation is consistent with that of Small et al. (1999) who found that in an alpine region of Wyoming, rates of regolith production beneath a cover of colluvium were nearly twice as fast as on exposed bedrock surfaces.

Lower nuclide concentrations in the sampled colluvium could be the result of cosmic-ray shielding by material now eroded, as nuclide production rates are lower at depth than at the surface. However, to account for the nearly two-fold difference between nuclide concentrations of the bedrock and the colluvium, would require a colluvium depth of  $\sim 70 \text{ cm}$ , which is unlikely on the steep slopes of this sub-basin and far thicker than we observed. More likely, moisture from infrequent precipitation is stored and held in contact with bedrock for a longer period of time

Table 2

Concentrations of  $^{10}\text{Be}$  and test of statistical differences between concentrations in geomorphic features of southwest sub-basin, Yuma Wash

Geomorphic feature	Mean $\pm$ standard error $^{10}\text{Be}$ measured ( $10^5 \text{ atoms g}^{-1}$ )	Statistical difference at 90% confidence						
		<i>n</i>	Bedrock outcrop	Hillslope colluvium	Basin fill	All channel	Upper channel	Lower channel
Bedrock outcrops	$2.73 \pm 0.28$	3	–	Yes	Yes	Yes	Yes	Yes
Hillslope colluvium	$1.38 \pm 0.15$	3	Yes	–	No	No	No	Yes
Basin fill	$1.16 \pm 0.07$	4	Yes	No	–	Yes	Yes	Yes
Channel seds (all)	$1.44 \pm 0.09$	5	Yes	No	Yes	–	–	–
Upper channel (YPG-11, 12, and 13)	$1.56 \pm 0.10$	3	Yes	No	Yes	–	–	Yes
Lower channel (YPG-14 and 15)	$1.26 \pm 0.02$	2	Yes	Yes	Yes	–	Yes	–

Average  $^{10}\text{Be}$  concentrations calculated by first averaging grain-size fractions of each sample then averaging together the samples representing each feature.

Statistical differences were determined at 90% confidence using independent *t*-tests and assuming unequal variances.

beneath a cover of colluvium than on exposed bedrock surfaces. This longer period of contact facilitates the chemical and mechanical weathering of the sub-colluvial rock (Gilbert, 1877; Wahrhaftig, 1965; Twidale, 1983; Bull, 1991; Small et al., 1999). More rapid weathering of sub-colluvial bedrock compounded with the high percentage of sub-basin area covered with a thin mantle of colluvium ( $\sim 70\%$ ), suggest that sub-colluvial bedrock weathering is the dominant source of sediment to the southwest fork of Yuma Wash. For all surfaces covered with colluvium, a basin-wide nuclide-based sediment generation rate estimate ( $73 \pm 8 \text{ g m}^{-2} \text{ year}^{-1}$ ) multiplied by the basin area with colluvial cover ( $\sim 5.5 \text{ km}^2$ ) yields a yearly sediment generation rate of  $40 \times 10^4 \text{ kg year}^{-1}$  compared to  $9.6 \times 10^4 \text{ kg year}^{-1}$  calculated for bedrock outcrop areas ( $40 \pm 9 \text{ g m}^{-2} \text{ year}^{-1}$  over  $\sim 2.4 \text{ km}^2$ ).

Comparison of the average  $^{10}\text{Be}$  concentration in southwest sub-basin channel sediment to concentrations in source areas is consistent with sub-colluvial weathering and downslope movement of hillslope colluvium as the dominant source of channel sediment. The average  $^{10}\text{Be}$  concentration in sediment of the southwest sub-basin channel ( $1.44 \pm 0.09 \times 10^5 \text{ atoms g}^{-1}$ ,  $n=5$ ), is indistinguishable (Table 2) from that measured in the hillslope colluvium ( $1.38 \pm 0.15 \times 10^5 \text{ atoms g}^{-1}$ ,  $n=3$ ), but is significantly lower than that measured in the bedrock outcrops ( $2.73 \pm 0.28 \times 10^5 \text{ atoms g}^{-1}$ ,  $n=3$ ).

In its lower reaches, the southwest sub-basin channel cuts through basin fill stored in terraces of interbedded alluvium and colluvium. Two profiles of this channel-cut basin fill (YPG-10 and YPG-26) show no significant nuclide concentration trends with depth (Fig. 7). Field observations of collapsed channel walls indicate that these deposits are an important source of sediment to the lower reaches of the channel. However, the average  $^{10}\text{Be}$  concentration of the basin fill ( $1.16 \pm 0.07 \times 10^5 \text{ atoms g}^{-1}$ ) is statistically less than (Table 2) the average concentration of  $^{10}\text{Be}$  measured in the channel sediment ( $1.44 \pm 0.09 \times 10^5 \text{ atoms g}^{-1}$ ).

Analysis of the spatial distribution of the channel sediment data reveals more detail about the dynamics of sub-basin sediment generation, storage, and transport. In the upper reaches of the southwest sub-basin channel (YPG-11, 12, and 13), average concentrations of nuclides in the channel sediment ( $1.56 \pm 0.10 \times 10^5$

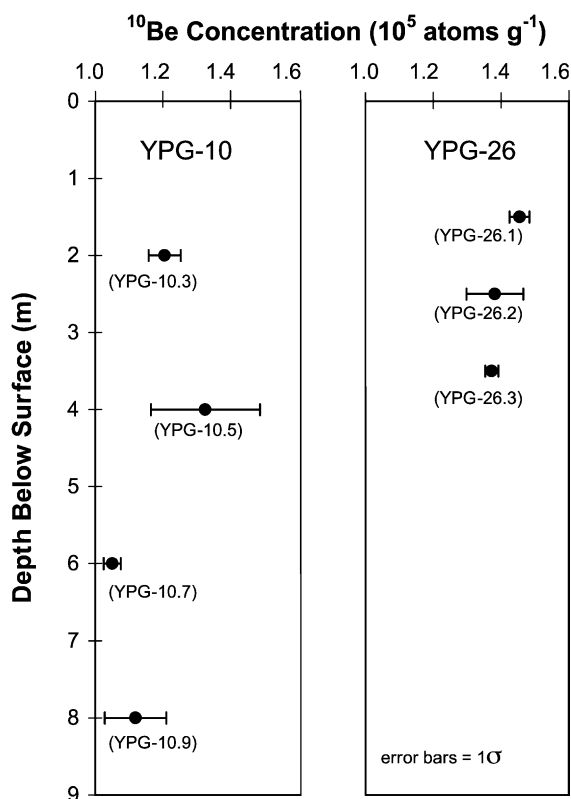


Fig. 7.  $^{10}\text{Be}$  concentrations plotted against depth for profiles measured in two basin fill deposits (YPG-10 and YPG-26) along the channel of the southwest sub-basin. No significant depth-related trends are evident.

$\text{atoms g}^{-1}$ ) are significantly higher than the average concentration in the lower reaches (YPG-14 and 15 average  $1.26 \pm 0.02 \times 10^5 \text{ atoms g}^{-1}$ ) indicating different sediment sources. Field observations suggest that in the upper reaches, sediment is derived from either weathering of bedrock beneath a cover of colluvium or by weathering of exposed bedrock outcrops (near- and in-channel sediment storage is negligible above YPG-14). In lower reaches, there are few direct pathways for hillslope sediment to be delivered to the channel, thus the channel sediments are derived primarily from either channel cutting of basin fill material in the fluvial terraces or from channel alluvium delivered from upstream. These observed sediment sources are consistent with our nuclide measurements.

In upper channel sediment, the average  $^{10}\text{Be}$  concentration ( $1.56 \pm 0.10 \times 10^5 \text{ atoms g}^{-1}$ ) is between that of the bedrock ( $2.73 \pm 0.28 \times 10^5 \text{ atoms g}^{-1}$ ) and

colluvium ( $1.38 \pm 0.15 \times 10^5$  atoms  $\text{g}^{-1}$ ) sources. From these concentrations we estimate relative contributions of roughly 13% bedrock and 87% colluvium to the upper channel alluvium, further supporting our conclusion that weathering of bedrock beneath coluvial cover is the dominant source of sediment to the channel. In the lower reaches, the average  $^{10}\text{Be}$  concentration ( $1.26 \pm 0.02 \times 10^5$  atoms  $\text{g}^{-1}$ ) is between that of the upstream channel alluvium ( $1.56 \pm 0.10 \times 10^5$  atoms  $\text{g}^{-1}$ ) and the channel basin fill ( $1.16 \pm 0.07 \times 10^5$  atoms  $\text{g}^{-1}$ ) sources. We estimate relative contributions of roughly 25% upstream alluvium and 75% basin fill to the downstream channel alluvium.

Although there are statistical differences between nuclide concentrations of the geomorphic features throughout the basin, the nuclide concentration of the lower channel alluvium is within one standard deviation of all other features excluding the bedrock outcrops. Additionally, the southwest sub-basin data illustrate that as sediment is transported through the basin it is mixed with sediment from different source areas. This mixing of the southwest fork sediment reservoirs implies that  $^{10}\text{Be}$  and  $^{26}\text{Al}$  concentrations of sediment leaving the sub-basin are representative of nuclide concentrations from throughout the sub-basin drainage. From nuclide concentrations meas-

ured near the sub-basin outlet (YPG-15), we calculate average rates of sediment generation and denudation for the southwest sub-basin (Table 3). Results from this sub-basin justify our assumption that channel sediments leaving small, upland sub-basins throughout the Yuma Wash Drainage represent average nuclide concentrations throughout each sub-basin.

#### 4.3. Main drainage basin

By measuring nuclide concentrations from tributaries and along the main stem of Yuma Wash (Fig. 1), we identify sediment source areas and find evidence for long-term trends in sediment transport. In the upper reaches of Yuma Wash (above YPG-19), a simple mixing model, which scales sediment contribution by sub-basin drainage area and nuclide-determined sediment generation rates (Table 4), predicts  $^{10}\text{Be}$  and  $^{26}\text{Al}$  concentrations in the main stem of Yuma Wash ( $1.9$  and  $12.0 \times 10^5$  atoms  $\text{g}^{-1}$ , respectively) consistent with the concentrations measured at YPG-19 ( $1.8 \pm 0.09$  and  $11.4 \pm 1.3 \times 10^5$  atoms  $\text{g}^{-1}$ , respectively). In the upper reaches of Yuma Wash, where sediment storage is minimal, our data demonstrate the utility of  $^{10}\text{Be}$  and  $^{26}\text{Al}$  as sediment-source tracers.

In downstream reaches, as sediment storage increases, our simple mixing model is inconsistent with

Table 3  
Sediment generation and denudation rates for Yuma Wash Drainage, Arizona

	This study			Sediment-cosmogenic based estimates from other regions					
	Main stem <sup>a</sup> channel sediment	SW sub-basin <sup>a</sup> channel sediment	Average <sup>a</sup> all sub-basins	Nahal Yael, <sup>b</sup> Israel	Arroyo <sup>c</sup> Chavez, New Mexico	Fort Sage <sup>d</sup> Mts (A), California	Fort Sage <sup>d</sup> Mts (B), California	Wind River <sup>c</sup> Range, Wyoming	
Sediment generation rate ( $\text{g m}^{-2} \text{ year}^{-1}$ )	$^{10}\text{Be}$	$101 \pm 10$	$73 \pm 8$	$81 \pm 5$	$78 \pm 16$	$273 \pm 62$	$162 \pm 38$	$97 \pm 24$	$39 \pm 11$
	$^{26}\text{Al}$	$100 \pm 11$	$68 \pm 8$	$81 \pm 8$	$70 \pm 16$	$281 \pm 73$	–	–	$35 \pm 11$
Denudation rate ( $\text{m Ma}^{-1}$ )	$^{10}\text{Be}$	$38 \pm 4$	$27 \pm 3$	$30 \pm 2$	$29 \pm 6$	$101 \pm 23$	$60 \pm 14$	$36 \pm 9$	$14 \pm 4$
	$^{26}\text{Al}$	$37 \pm 4$	$25 \pm 3$	$30 \pm 3$	$26 \pm 6$	$104 \pm 27$	–	–	$13 \pm 4$

<sup>a</sup> Denudation rates calculated using formulation of Bierman and Steig (1996) and production rates of Nishiizumi et al. (1989), scaled for latitude and elevation according to Lal (1991), and not scaled for slope due to small average slopes (<20%). Conversion between denudation and sediment generation based on densities of  $2.7 \text{ g cm}^{-3}$  for bedrock. Rates for main stem calculated using nuclide concentrations from samples collected at location YPG-2 weighted by size fraction relative percent by weight. Rates for SW sub-basin calculated using nuclide concentrations from samples collected at locations YPG-14 and YPG-15 weighted by size fraction relative percent by weight. Average of all sub-basins calculated from samples collected at YPG-4, -15, -18, -20, -21, -22, and -27 weighted by sub-basin drainage area.

<sup>b</sup> Clapp et al. (2000)—site with similar climate, elevation, and lithologies.

<sup>c</sup> Clapp et al. (1997, 2001)—site with higher elevation ( $\sim 2000$  m), wetter climate (377 mm), less resistant bedrock.

<sup>d</sup> Granger et al. (1996) used both  $^{10}\text{Be}$  and  $^{26}\text{Al}$  to calculate erosion rates in two catchments (A and B)—site  $\sim 1300$  m.

<sup>e</sup> Small et al. (1999)—site with higher elevation ( $\sim 3600$  m) and thicker colluvial cover ( $\sim 90$  cm).

Table 4  
Mixing model results for area upstream from YPG-19 at Yuma Wash, Arizona

Sample location (sub-basin)	Sub-basin drainage area (km <sup>2</sup> )	Sediment generation rate (g m <sup>-2</sup> year <sup>-1</sup> )	Sediment mass (10 <sup>6</sup> kg year <sup>-1</sup> )	%Total mass	<sup>10</sup> Be measured concentration (10 <sup>5</sup> atoms g <sup>-1</sup> )	<sup>26</sup> Al measured concentration (10 <sup>5</sup> atoms g <sup>-1</sup> )	<sup>10</sup> Be erosion-weighted average (10 <sup>5</sup> atoms g <sup>-1</sup> )	<sup>26</sup> Al erosion-weighted average (10 <sup>5</sup> atoms g <sup>-1</sup> )
YPG-21	29.3	59	1.7	42	2.19	14.3	0.92	5.99
YPG-27	18.6	80	1.5	36	1.66	10.4	0.60	3.74
YPG-22	5.8	88	0.5	12	1.53	9.1	0.19	1.13
YPG-20	5.8	70	0.4	10	1.92	11.6	0.19	1.14
Erosion-weighted average nuclide concentration upstream from YPG-19							1.9	12.0
Measured nuclide concentration at YPG-19 confluence							1.8 ± 0.1	11.4 ± 1.3

Erosion-weighted averages calculated by: (1) multiplying sub-basin area by nuclide-determined sediment generation rate to get annual mass of sediment per basin; (2) calculating the percentage of the total mass from all four sub-basins; (3) multiplying %total mass per basin by nuclide concentration and summing the results.

measurements in Yuma Wash. Along the 26-km of the Wash, we find a regular, downstream decrease in nuclide concentrations, well modeled by an exponential equation (Fig. 8). Additionally, at several locations we find that the nuclide concentrations measured in the main stem of the Yuma Wash appear to be slightly

lower (although not significant at 2σ) than those of all tributaries upstream (Fig. 1). Down basin decreases in elevation (average elevation above sample site) and associated increases in atmospheric shielding (Lal, 1991), could account for only ~ 14% of the ~ 50% down-basin decrease in nuclide concentrations. These

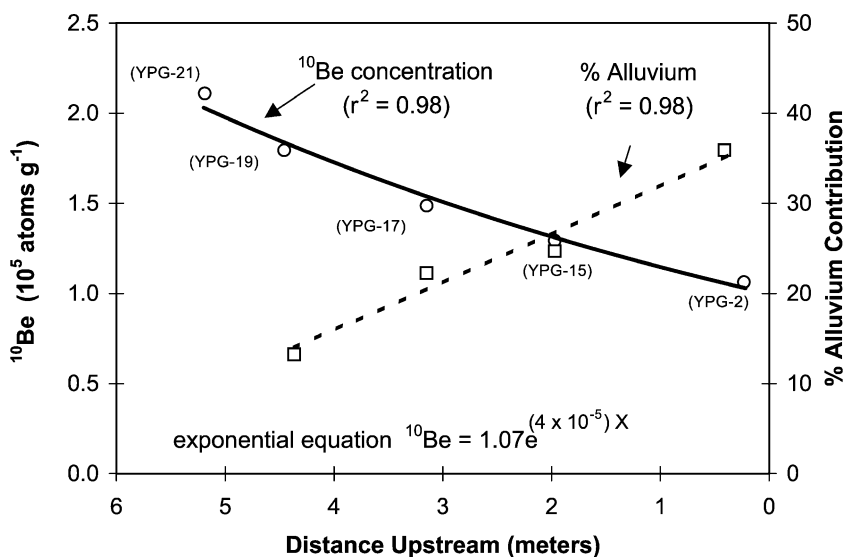


Fig. 8. Trend of sample distance downstream versus <sup>10</sup>Be concentrations along with results of mixing model (% alluvium) for the main stem of Yuma Wash. Open circles represent <sup>10</sup>Be concentrations at locations designated in parentheses (see Fig. 1 for sample locations). The downstream trend is well modeled by an exponential equation. The mixing model described in Table 4 was also used to predict nuclide concentrations at specific confluences along the main stem of Yuma Wash. Model concentrations higher than measured concentrations indicate the addition of low-nuclide alluvium (0.84 × 10<sup>5</sup> atoms g<sup>-1</sup>, YPG-16) to the channel. Open squares above represent the percentage of low-nuclide alluvium necessary to equilibrate model and measured concentrations. The percentage of low-nuclide alluvium added at each point along the main stem increases downstream as nuclide concentrations of main stem channel sediment decrease.

observations together, suggest an additional and unaccounted for source of low-nuclide concentration sediment to the channel.

Field observations of the Yuma Wash channel cutting into basin fill sediments stored in terraces suggest the source of low-nuclide concentration sediment. To determine the nuclide concentration of this basin fill, we sampled sediment from a sub-basin that is wholly contained within the basin-fill alluvium (YPG-16). This sample provides an integrated measurement of the nuclide concentrations through a stream-cut cross-section of basin alluvium. The average  $^{10}\text{Be}$  concentration we determine for the basin fill ( $0.84 \pm 0.05 \times 10^5$  atoms  $\text{g}^{-1}$ ) is substantially lower than sediment supplied directly from the upland sub-basins ( $1.28 \pm 0.05$  to  $2.19 \pm 0.08 \times 10^5$  atoms  $\text{g}^{-1}$ ). There are several possible explanations for the low-nuclide abundance in the basin fill. First, if the deposits are old ( $>3$  to  $4$  Ma), inherited nuclide abundances would have decayed to near zero (deposits as great as 10-m thick would shield much of the material from incoming cosmic rays), and the nuclide concentrations we measure have accumulated since deposition as the basin fill eroded. Alternatively, the alluvium may have been generated at a period of time when the basin was eroding more quickly and average, basin-wide nuclide concentrations were lower. The latter scenario would require sediment generation rates as high as  $160 \pm 36$   $\text{g m}^{-2} \text{ year}^{-1}$  at the time of basin-fill deposition.

We use the basin-fill concentrations measured at YPG-16 to calculate mixing ratios between highly dosed sediment coming from resistant highlands and less-dosed material coming from poorly consolidated and highly dissected basin fill (Fig. 8). As the valley fill thickens downstream and sediment storage becomes more prevalent, our data suggest a downstream increase in sediment contribution from channel incision of the basin fill. Where Yuma Wash discharges to the Colorado River, we estimate over 40% of the sediment it transports has been recycled through the basin fill.

In addition to low-nuclide concentration sediment derived from basin fill, it is likely that lower concentration sediment from more rapidly eroding, quartz-rich, granitic sub-basins contributes to lower nuclide concentrations of the main-stem alluvium. However, only the southern third of the Yuma Wash drainage is influenced by granitic sub-basins and only the lowest of

our main stem sampling locations (YPG-2) could be influenced. Upstream from YPG-2, YPG-5 receives sediment from only a few low-order tributaries emanating from granitic terrains while receiving most of its sediment from the main stem as it leaves the rhyolitic areas. All other main stem samples are wholly contained within the rhyolitic terrain.

#### 4.4. Rates of sediment generation and denudation

From the Yuma Wash data, we calculate rates of sediment generation and denudation (Table 3). Nuclide concentrations measured in the southwest sub-basin support our assumption that sediment exported from small, upland drainage basins is well mixed and representative of sediment generated throughout those basins. We therefore use an average of nuclide-determined sediment generation rates from all sampled basins to estimate the basin-wide sediment generation and denudation rates ( $81 \pm 5$   $\text{g m}^{-2} \text{ year}^{-1}$  and  $30 \pm 2$   $\text{m Ma}^{-1}$ , respectively) for the entire Yuma Wash drainage basin (Table 3). Our rates should be considered minimum estimates as dissolution of non-quartz minerals in regolith can cause concentration of quartz and under-estimation of sediment generation rates (Small et al., 1999). However, quartz enrichment should be minimal in the arid climate and resistant bedrock of Yuma Wash. We also determine basin-wide rates using only nuclide concentrations measured in sediment from near the mouth of Yuma Wash (YPG-2) and find the main stem estimates ( $101 \pm 10$   $\text{g m}^{-2} \text{ year}^{-1}$  or  $38 \pm 4$   $\text{m Ma}^{-1}$ ) are slightly higher ( $\sim 25\%$ ) than the estimates from averaging all sub-basins. This dissimilarity between rates suggests that at the larger scale, where sediment storage is significant, nuclide concentrations in alluvium exported from the basin appear to slightly overestimate basin-wide rates of sediment generation and denudation. The higher rate of denudation we calculate from the main channel sediment analysis suggests that sediment is currently being exported from the basin more quickly than it is being generated in the uplands, an assertion supported by field observations of active stream bank cutting and highly dissected alluvial fan surfaces throughout the basin.

Although the rates calculated from sub-basins and the main stem are statistically separable (at 90% confidence), they are within two standard deviations and

well within an order of magnitude. The similarity between the two results suggests that at the larger scale, nuclide concentrations in channel alluvium exported from the basin may be used as a rough approximation of basin-wide rates of sediment generation and denudation.

## 5. Implications

Cosmogenic nuclide concentrations, measured in samples collected from individual geomorphic features in the southwest sub-basin, indicate that sub-colluvial weathering of bedrock generates sediment more quickly ( $73 \pm 8 \text{ g m}^{-2} \text{ year}^{-1}$ ) than the weathering of exposed bedrock outcrops ( $40 \pm 9 \text{ g m}^{-2} \text{ year}^{-1}$ ). This difference indicates that the processes of chemical and mechanical weathering by water, held in contact with bedrock, speed the conversion of bedrock to soil in arid environments (Gilbert, 1887; Twidale, 1983; Bull, 1991; Small et al., 1999).

The basin-wide rates of sediment generation ( $81 \pm 5 \text{ g m}^{-2} \text{ year}^{-1}$ ) and denudation ( $30 \pm 2 \text{ m Ma}^{-1}$ ) (Table 3) calculated for the uplands supplying sediment to Yuma Wash, are consistent with rates determined by other researchers. Judson and Ritter (1964) calculated denudation rates for 28 major drainages throughout the United States, generally ranging from 10 to 150  $\text{m Ma}^{-1}$ . We expect that our rates should fall on the lower end of this scale because of the arid climate and erosion-resistant bedrock underlying Yuma Wash. Rates of sediment generation and denudation at Yuma Wash are similar to estimates from a basin of similar climate, elevation and lithology in the Negev Desert of southern Israel (Clapp et al., 2000) and are slightly lower than those calculated for a basin at Arroyo Chavez, New Mexico (Clapp et al., 1997, 2001) and basins in the Fort Sage Mountains of California (Granger et al., 1996) where the climates are wetter and the elevations higher (Table 3). Our rate estimates are approximately twice those calculated by Small et al. (1999) in the Wind River Range, Wyoming, where samples were collected primarily from summit flats ( $< 10^\circ$  slopes) as opposed to the steep slopes ( $10^\circ$  to  $30^\circ$ ) of the Yuma Wash uplands.

Independence of nuclide concentration and sediment grain size is indicative of sediment transport and production processes within arid regions. Arid-region

channels transport sediment in discrete pulses before rapidly depositing poorly sorted material. Thus, such channels are likely to leave behind isotopically homogenous sediment as differences in transport times for different size materials are minimal.

Nearly homogenous nuclide concentrations in the southwest sub-basin sediments imply that average sediment storage is so short-lived that stored sediment cannot accumulate detectable amounts of  $^{10}\text{Be}$  or  $^{26}\text{Al}$  following deposition. This isotopic homogeneity we observe in sediment of small, upland basins suggests that channel sediment nuclide concentrations are representative of nuclide concentrations throughout such basins.

Cosmogenic nuclide concentrations along the length of the main stem and from individual tributaries of Yuma Wash can be used to determine significant sources of sediment to the channel. Mixing models suggest that in the upper reaches of the wash, sediment supply is predominantly from low-order tributaries transporting material generated by erosion of the uplands. Lower in the basin, where the channel cuts through poorly consolidated valley alluvium, sediment incorporated from long-term storage becomes an increasingly significant component of the channel load. We use nuclide concentrations to estimate that as much as 40% of sediment exported from Yuma Wash is recycled from the stored basin alluvium.

Basin-wide rates of sediment generation and denudation calculated by averaging rates from all sub-basins are different than rates calculated from nuclides measured in alluvium near the mouth of Yuma Wash. The difference between the rates again suggests that stored sediment is currently being eroded from the basin. Our data clearly show that the effects of sediment storage can be detected and may become even more significant in larger basins with greater storage than Yuma Wash.

## Acknowledgements

Supported by the US Department of Defense, Army Research Office-Terrestrial Sciences (Grants DAA G559710180 and DAAH049610036), NSF Grant EAR-9628559, and Department of Energy contract #W-7405-ENG-48. We thank V. Morrill, K. Nichols, M. Abbott, and C. Massey for assistance in the field, S.

Nies, J. Southan, and B. Copans for assistance in the laboratory, and J. Sevee and P. Maher for additional support.

## References

- Ahnert, F., 1970. Functional relationships between denudation, relief, and uplift in large mid-latitude drainage basins. *Am. J. Sci.* 268, 243–263.
- Ayers-Associates, 1996. Geomorphic, Hydrologic, and Vegetation Characterization and Base-Line Conditions of Yuma Wash. U.S. Army Corps of Engineers Waterways Experimental Station, Vicksburg, Mississippi and Conservation Program U.S. Army Yuma Proving Grounds, Yuma, AZ, Rpt. 92-0904.01, 398 pp.
- Bierman, P., Steig, E., 1996. Estimating rates of denudation and sediment transport using cosmogenic isotope concentrations in sediment. *Earth Surf. Processes Landforms* 21, 125–139.
- Brown, T.B., Stallard, R.F., Larsen, M.C., Raisbeck, G.M., Francoise, Y., 1995a. Denudation rates determined from accumulation of in situ-produced  $^{10}\text{Be}$  in the Luquillo Experimental Forest, Puerto Rico. *Earth Planet. Sci. Lett.* 129, 193–202.
- Brown, E.T., Stallard, R.F., Larsen, M.C., Raisbeck, G.M., Francoise, Y., 1995b. Evidence for muon-induced production of  $^{10}\text{Be}$  in near surface rocks from the Congo. *Geophys. Res. Lett.* 22, 703–706.
- Bull, W.B., 1991. *Geomorphic Responses to Climate Change*. Oxford Univ. Press, New York, 326 pp.
- Clapp, E.M., Bierman, P.B., Pavich, M., Caffee, M., 1997. Rates of erosion determined using in situ-produced cosmogenic isotopes in a small arroyo basin, northwestern New Mexico. *Geol. Soc. Am. Abstr. Prog.* 29, 281.
- Clapp, E.M., Bierman, P.R., Schick, A.P., Lekach, J., Enzel, Y., Caffee, M., 2000. Sediment yield exceeds sediment production in arid region drainage basins. *Geology* 28, 995–998.
- Clapp, E.M., Bierman, P.R., Nichols, K.K., Pavich, M., Caffee, M., 2001. Rates of sediment supply to arroyos from upland erosion determined using in situ-produced cosmogenic  $^{10}\text{Be}$  and  $^{26}\text{Al}$ . *Quaternary Research* 55, 235–245.
- Clark, D.H., Bierman, P.R., Larsen, P., 1995. Improving in situ cosmogenic chronometers. *Quat. Res.* 44, 366–376.
- Dohrenwend, J.C., Bull, W.B., McFadden, L.D., Smith, G.I., Smith, R.S.U., Wells, S.G., 1991. Quaternary geology of the basin and range province in California. In: Morrison, R.B. (Ed.), *Quaternary Nonglacial Geology, Conterminous U.S.* Geol. Soc. America. The Geology of North America, vol. K-2, pp. 353–371.
- Gilbert, G.K., 1877. *Geology of the Henry Mountains (Utah)*, U.S. Geographical and Geological Survey of the Rocky Mountains Region, 170 pp.
- Granger, D.E., Kirchner, J.W., Finkel, R., 1996. Spatially averaged long-term erosion rates measured from in-situ produced cosmogenic nuclides in alluvial sediment. *J. Geol.* 104, 249–257.
- Judson, S., 1968. Erosion of the land, or what's happening to our continents? *Am. Sci.* 56, 356–374.
- Judson, S., Ritter, D.F., 1964. Rates of regional denudation in the United States. *J. Geophys. Res.* 69, 3395–3401.
- Kohl, C.P., Nishiizumi, K., 1992. Chemical isolation of quartz for measurement of in-situ-produced cosmogenic nuclides. *Geochem. Cosmochem. Acta* 56, 3583–3587.
- Lal, D., 1988. In situ-produced cosmogenic isotopes in terrestrial rocks. *Annu. Rev. Earth Planet. Sci.* 16, 355–388.
- Lal, D., 1991. Cosmic ray labeling of erosion surfaces: in situ production rates and erosion models. *Earth Planet. Sci. Lett.* 104, 424–439.
- Laronne, J., Reid, I., 1993. Very high rates of bedload sediment transport by ephemeral desert rivers. *Nature* 366, 148–150.
- Laronne, J., Reid, I., Yitshak, Y., Frostick, L., 1994. The non-layering of gravel streambeds under ephemeral flood regimes. *J. Hydrol.* 159, 353–363.
- Meade, R.H., 1969. Errors in using modern stream-load data to estimate natural rates of denudation. *Geol. Soc. Am. Bull.* 80, 1265–1274.
- Meade, R.H., 1988. Movement and storage of sediment in river systems. In: Lerman, A., Meybeck, M. (Eds.), *Physical and Chemical Weathering in Geochemical Cycles*. Kluwer Academic Publishing, Amsterdam, pp. 165–179.
- Nishiizumi, K., Winterer, E.L., Kohl, C.P., Klein, J., Middleton, R., Lal, D., Arnold, J.R., 1989. Cosmic ray production rates of  $^{10}\text{Be}$  and  $^{26}\text{Al}$  in quartz from glacially polished rocks. *J. Geophys. Res.* 94, 17907–17915.
- Ott, R.L., 1993. *An Introduction to Statistical Methods and Data Analysis*. Wadsworth Publishing, Belmont, CA, 1051 pp.
- Pinet, P., Souriau, M., 1988. Continental erosion and large-scale relief. *Tectonics* 7, 563–582.
- Reid, I., Laronne, J., 1995. Bedload sediment transport in an ephemeral stream and a comparison with seasonal and perennial counterparts. *Water Resour. Res.* 31, 733–781.
- Reynolds, S.J., 1988. *Geologic Map of Arizona*. Arizona Geological Survey.
- Saunders, I., Young, A., 1983. Rates of surface processes on slopes, slope retreat, and denudation. *Earth Surf. Processes Landforms* 8, 473–501.
- Small, E.E., Anderson, R.S., Hancock, G.S., 1999. Estimates of the rate of regolith production using  $^{10}\text{Be}$  and  $^{26}\text{Al}$  from an alpine slope. *Geomorphology* 27, 131–150.
- Trimble, S.W., 1977. The fallacy of stream equilibrium in contemporary denudation studies. *Am. J. Sci.* 277, 876–887.
- Twidale, C.R., 1983. The research frontier and beyond: granitic terrains. *Geomorphology* 7, 187–223.
- Wahrhaftig, C., 1965. Stepped topography of the southern Sierra Nevada, CA. *Geol. Soc. Am. Bull.* 76, 1165–1190.